



Fermi National Accelerator Laboratory

FERMILAB-Pub-83/97-THY
October, 1983

Twisted Reduced Chiral Models at large N

SUMIT R.DAS

Fermi National Accelerator Laboratory

Batavia, Illinois 60510

and

JOHN B.KOGUT

Department of Physics

University of Illinois at Urbana-Champaign

Urbana, Illinois 61801.



ABSTRACT

We construct and study the twisted reduced $SU(N) \times SU(N)$ chiral model in two dimensions. The equivalence of the reduced model to the field theory is established by examining the Dyson-Schwinger equations and weak coupling perturbation expansion. We evaluate the internal energy and two-point correlation function by extensive Monte-Carlo simulations for $N=12, 24$ and 36 . We find a non-analyticity near the weak coupling edge of the crossover region in which the system flips back and forth between the "normal" state and one characterised by a strongly disordered correlation function.

INTRODUCTION

It has been shown recently that at $N=\infty$ field theories with $SU(N)$ or $O(N)$ internal symmetry become equivalent to matrix models living at a single site [1-3]. These reduced models have made numerical simulations of large N theories practicable. There are two distinct types of reduced models which reproduce the corresponding field theory. The first class, known as Quenched Eguchi-Kawai (QEK) models represents translations in the diagonal part of the internal symmetry group [2]. However, particularly for gauge theories, this turns out to be rather cumbersome, and a much simpler version has been proposed - the Twisted Eguchi-Kawai (TEK) models. In TEK models, translations are represented by internal symmetry matrices which form a 't Hooft algebra.

The TEK models are particularly well-suited for numerical computations. Apart from their simplicity, they have a weaker dependence of N on the volume of the system. For QEK models to work, one must have $N \geq L^d$ (where L is the size of the box in which the parent field theory is defined), while for TEK models one has $N=L^{d/2}$. This means that finite size effects are less severe in TEK models; in fact, the finite size corrections are of the same order as the leading large N corrections.

In this paper we shall construct and study the twisted reduced $SU(N) \times SU(N)$ chiral model in two dimensions. The two dimensional chiral model is believed to be in the same

universality class as the four dimensional gauge theory [4]. In fact, studies of the $N=3$ model vindicate this belief [5].

We have performed extensive Monte-Carlo simulations of the TEK chiral model for several values of N . The internal energy and the two-point correlation function were measured. While the dependence of the internal energy on the coupling is in good agreement with the results of the strong and weak coupling expansions at the respective ends, we find evidence for a strong non-analyticity in intermediate coupling. This occurs near the weak coupling edge of the cross-over region. The system switches back and forth between two states: one characterised by a weakly disordered correlation function, the other exhibiting strong disorder. Such strong disorder (with correlation functions actually turning negative for large separations) is totally out of tune with the general trend as one goes from strong to weak coupling. The physics of this peculiar behaviour is not clear at the moment.

The QEK version of the chiral model has been studied earlier in the literature [6]. In this case a first order phase transition in the cross-over region has been reported. Our results do not contain any evidence for such a transition, although the convergence is definitely slow in this region. Our simulations have also accumulated 10-100 times the data of previous studies and, since we study TEK models, the finite size effects are considerably smaller ($\sim 1/5$) than previous studies.

In Section II we define the model. Section III

contains a brief discussion of the equivalence of this model with the parent field theory via Dyson-Schwinger equations and weak coupling perturbation theory. In Section IV we summarise the results of our numerical investigation.

II. THE MODEL.

The field theory we shall consider is defined on a square lattice by the action:

$$S = -\beta \sum_{x, \mu} \text{Tr} [U(x) U^\dagger(x+\mu) + h.c.] \quad \dots \quad (1)$$

The twisted model is obtained by applying the reduction prescription:

$$U(x) \rightarrow D(x) U D^\dagger(x)$$

$$D(x) \equiv \prod_{\mu=1}^2 (\Gamma_\mu)^{x_\mu} \quad \dots \quad (2)$$

where Γ_μ 's are traceless $SU(N)$ matrices satisfying the algebra:

$$\Gamma_\mu \Gamma_\nu = \exp\left(\frac{2\pi i}{N} n_{\nu\mu}\right) \Gamma_\nu \Gamma_\mu \quad \dots \quad (3)$$

The reduced action becomes:

$$S_R = -\beta \sum_{\mu} \text{Tr} (U \Gamma_\mu U^\dagger \Gamma_\mu^\dagger + h.c.) \quad \dots \quad (4)$$

The field theory is invariant under the symmetry $SU(N) \times SU(N)/\mathbb{Z}_N$:

$$U(x) \rightarrow P U(x) Q^\dagger$$

where P and Q are independent $SU(N)$ matrices. The reduced model (4) is, however, invariant under the symmetries:

$$U \rightarrow Z U$$

$$U \rightarrow S(Q) U S^\dagger(Q) \quad \dots \quad (5)$$

where z is an element of Z_N and $S(q)$ is given by:

$$S(q) = \prod_{\mu} (\Gamma_{\mu})^{q_{\mu}}, \quad q_{\mu} = \text{integer}$$

Expectation values of invariant quantities are obtained by applying the reduction prescription (2) and averaging over the ensemble defined by the reduced action S_R with a fixed value of the twist $n_{\mu\nu}$. Thus for a typical Green's function of the parent theory which respects the full symmetry:

$$G(x_i) = \text{Tr} \langle U(x_1) U^{\dagger}(x_2) \dots U(x_{n-1}) U^{\dagger}(x_n) \rangle \dots \quad (6)$$

the corresponding object in the reduced model is:

$$G_R(x_i) = \text{Tr} \langle D(x_1) U D^{\dagger}(x_1) D(x_2) U^{\dagger} D^{\dagger}(x_2) \dots \rangle_R \dots \quad (7)$$

where $\langle \rangle_R$ denotes average in the reduced model. The twists $n_{\mu\nu}$ are to be chosen so that the equivalence

$$G(x_i) = G_R(x_i)$$

holds.

III. EQUIVALENCE TO THE FIELD THEORY

The equivalence of the reduced model to the field theory may be established by considering Dyson-Schwinger equations obeyed by the Green's functions. These equations may be derived in the standard manner (see e.g. Ref[7]). Consider the following quantity in the parent field theory:

$$\begin{aligned} & \text{Tr} \langle \lambda_a U(x_1) U^\dagger(x_2) \dots \rangle \\ & = \frac{1}{Z} \int dU \exp[-\beta S] \text{Tr} [\lambda_a U(x_1) U^\dagger(x_2) \dots] \end{aligned} \quad \dots (8)$$

where λ_a are the generators of SU(N) normalised in the standard fashion. Now make a change of variables:

$$U(x_1) \rightarrow (1 + i\varepsilon \lambda_a) U(x_1) \quad \dots (9)$$

Under this change of variables, the measure is invariant and one has the following equation:

$$\begin{aligned} & \frac{\beta}{N} \sum_{\mu} \langle \frac{1}{N} \text{Tr} \{ [U(x_1) U^\dagger(x_2) \dots] [U(x_1) U^\dagger(x_1+\mu) - U(x_1+\mu) U^\dagger(x_1)] \} \rangle \\ & = \langle \frac{1}{N} \text{Tr} [U(x_1) U^\dagger(x_2) \dots U^\dagger(x_n)] \rangle + \\ & \sum_{\ell} \delta(x_1, x_\ell) \left\{ \frac{1}{N^2} \langle \text{Tr} [U(x_1) U^\dagger(x_2) \dots U^\dagger(x_{\ell-1})] \times \right. \\ & \quad \left. \text{Tr} [U(x_\ell) \dots U^\dagger(x_n)] \rangle \right. \\ & \quad \left. - \frac{1}{N^2} \langle \text{Tr} [U^\dagger(x_2) \dots U(x_{\ell-1})] \times \right. \\ & \quad \left. \text{Tr} [U(x_{\ell+1}) \dots U^\dagger(x_n)] \rangle \right\} \\ & \dots \dots (10) \end{aligned}$$

At $N \rightarrow \infty$ expectation values of products of invariant quantities factorise leading to a closed equation for quantities of the type $G(x_i)$:

$$\begin{aligned} & \frac{\beta}{N} \sum_{\mu} \langle \frac{1}{N} \text{Tr} \{ [U(x_1)U^\dagger(x_2)\dots] [U(x_1)U^\dagger(x_1+\mu) - U(x+\mu)U^\dagger(x_1)] \} \rangle \\ &= \langle \frac{1}{N} \text{Tr} [U(x_1)U^\dagger(x_2)\dots U^\dagger(x_n)] \rangle + \\ & \sum_l \delta(x_1, x_l) \left\{ \langle \frac{1}{N} \text{Tr} [U(x_1)U^\dagger(x_2)\dots U^\dagger(x_{l-1})] \rangle \langle \frac{1}{N} \text{Tr} [U(x_2)\dots U^\dagger(x_n)] \rangle \right. \\ & \quad \left. - \langle \frac{1}{N} \text{Tr} [U^\dagger(x_2)\dots U^\dagger(x_{l-1})] \rangle \langle \frac{1}{N} \text{Tr} [U(x_{l+1})\dots U^\dagger(x_n)] \rangle \right\} \end{aligned} \quad \dots (11)$$

For the reduced model one starts with the translate of (8):

$$\begin{aligned} & \text{Tr} \langle D(x_1) \lambda_a U D^\dagger(x_1) \cdot D(x_2) U D^\dagger(x_2) \dots \rangle \\ &= \frac{1}{Z} \int dU \exp[-\beta S_R] \text{Tr} [D(x_1) \lambda_a U D^\dagger(x_1) \dots] \end{aligned} \quad \dots (12)$$

and makes a change of variables:

$$U \rightarrow (1 + i\epsilon \lambda_a) U \quad \dots (13)$$

An identical procedure now leads to an equation which is just the translate of equation(10) apart from additional source terms of the generic form: (for $x_i \neq x_m$)

$$\begin{aligned} & \sum_{x_m} \left\{ \langle \text{Tr} D(x_m) U D^\dagger(x_1) D(x_2) \dots D^\dagger(x_{m-1}) \rangle \times \right. \\ & \quad \langle \text{Tr} D(x_1) U D^\dagger(x_m) \dots D^\dagger(x_n) \rangle \\ & \quad - \langle \text{Tr} D(x_m) D^\dagger(x_1) D(x_2) \dots D^\dagger(x_{m-1}) \rangle \times \\ & \quad \left. \langle \text{Tr} D(x_1) D^\dagger(x_m) D(x_{m+1}) U D^\dagger(x_{m+1}) \dots D^\dagger(x_n) \rangle \right\} \end{aligned} \quad \dots (14)$$

where factorisation property has been used. There are similar terms for $x_1 = x_m$; however, the equations for $G(x)$ also contain these terms. The reduced model is thus equivalent to the field theory only if these terms vanish for all β .

In extreme weak coupling ($\beta = \infty$), U is frozen to the unit matrix (or a Z_N -multiple of it) and the extra source terms involve traces like:

$$\text{Tr } D(x_m - x_1)$$

The condition that such traces be non-zero is easily seen to be:

$$n_{\mu\nu} (x_m - x_1)_\nu = p_\mu N \quad \dots (15)$$

where p_μ 's are integers. By an explicit calculation, it may be checked that (15) is also the condition for the source terms to be non-zero at strong coupling.

In two dimensions $n_{\mu\nu}$ is necessarily of the form $n_{\mu\nu} = n \epsilon_{\mu\nu}$. Then (15) becomes:

$$(x_m - x_1)_\mu = \frac{1}{n} \epsilon_{\mu\nu} p_\nu N \quad \dots (16)$$

Suppose, for a given integer L , $n = L^m$ and $N = L^{m+1}$. Then (16) shows that if the parent field theory is defined in a periodic box of size L , all pairs of points (x_1, x_m) for which the Dyson-Schwinger equations may differ for the two theories are actually the same point by periodicity.

To find the correct choice of m , we investigate the weak coupling expansion of the reduced model. One expands

around the vacuum:

$$U = \exp(i a / \sqrt{\beta}) \quad a^\dagger = a \quad (17)$$

The momenta are generated entirely from the internal degrees of freedom. this is seen by expanding a as follows:

$$a = \sum_q a(q) A(q)$$

where
$$A(q) = \prod_{\mu} (\Gamma_{\mu})^{k_{\mu}} \quad \dots \quad (18)$$

and
$$n_{\mu\nu} k_{\nu} = q_{\mu}$$

where the k_{μ} 's and q_{μ} 's are integers. Since Γ_{μ} 's are translation matrices in a periodic box of size L , $(\Gamma_{\mu})^L = 1$ and there are L^d independent $A(q)$'s in d dimensions. For these to form a complete basis for the N^2 degrees of freedom contained in a ,one must have $N=L^{d/2}$ which gives $N=L$ in two dimensions. A detailed analysis of the perturbation expansion (along the lines of Ref.[8]) shows that this is the only choice which lead to identical perturbation series for the reduced model and the field theory. We thus conclude that at least in the weak coupling and strong coupling regions the reduced model with $N=L$ is equivalent to the chiral field theory defined in a periodic box of size L . We shall assume that the equivalence persists for all coupling. The Γ_{μ} 's may be chosen to be the standard $N \times N$ 't Hooft twist matrices:

$$\begin{aligned} (\Gamma_1)_{ij} &= \delta_{i+1,j \pmod{N}} \quad \dots \quad (19) \\ (\Gamma_2)_{ij} &= \delta_{ij} \exp \left[\frac{2\pi i}{N} \left(j - \frac{1}{2} - \frac{N}{2} \right) \right] \end{aligned}$$

We record below the lowest order contributions to the internal energy E :

$$E \equiv \frac{1}{N} \sum_{\mu} \operatorname{Re} \left\{ \operatorname{Tr} (U \Gamma_{\mu} U^{\dagger} \Gamma_{\mu}^{\dagger}) \right\} \dots (20)$$

in the strong and weak coupling expansions:

$$\langle E \rangle = \frac{2}{N} \beta + O\left(\frac{\beta^2}{N^2}\right) \quad \frac{\beta}{N} \ll 1 \quad \dots (21)$$

$$\langle E \rangle = 2 - \frac{N}{4\beta} + O\left(\frac{N^2}{\beta^2}\right) \quad \frac{\beta}{N} \gg 1$$

IV. NUMERICAL RESULTS

We have performed Monte-Carlo simulations of the model described above for $N=12, 24$ and 36 . The matrix U was updated by left multiplication with a random $SU(N)$ matrix which has non-trivial entries only in a $SU(2)$ subgroup. One sweep corresponds to going through all the $SU(2)$ subgroups. The updating matrix was adjusted to obtain an acceptance rate of approximately 50% in the standard Metropolis algorithm. We measured the internal energy defined in equation (13) and the two point correlation function:

$$G(x) = \frac{1}{N} \text{Re} \langle \text{Tr} [U(\Omega)^x U^\dagger(\Omega^\dagger)^x] \rangle \dots (22)$$

The internal energy was monitored in block averages over every ten sweeps, while correlation functions were measured in block averages over every 100 sweeps. Typically several thousand sweeps were made; in the cross-over region we often went through as many as 25,000 sweeps.

Figures (1) and (2) show the internal energies as functions of the coupling for $N=24$ and $N=36$ respectively. The lines represent the lowest order strong and weak coupling results. The agreement with our data is rather good. There is a sharp crossover in the vicinity of $\beta/N = 0.3$. To probe the physics in the cross-over region we made long runs with both ordered and disordered starts. Contrary to previous reports about the QEK chiral model, we do not

find any evidence for a first order phase transition. The convergence to equilibrium is rather slow in this region, but the histories of internal energy for both hot and cold starts converge to the same value. Figure (3) shows a typical history at very weak coupling (data points are block averages over 500 sweeps) Figures (4) and (5) show the corresponding behaviour in the cross-over regime.

As we proceed towards the weak coupling edge of the cross-over, we observe evidence for some non-analyticity. This shows up markedly in the behaviour of the correlation function and weakly in the internal energy. In Figure (6) we show the behaviour of the correlation function for various values of the coupling excluding the region of non-analyticity mentioned above. The correlation length increases smoothly with β . In a region between $\beta/N=0.48$ and $\beta/N=0.55$ the correlation function exhibits two distinct types of behaviour as we follow the history over many sweeps. We have studied this region quite extensively with very long runs. Typically, the system would appear to settle down after a few hundred sweeps with the correlation function behaving in a fashion essentially similar to that at lower β . However, after some time (usually after 4000 or 5000 sweeps) the system suddenly flips over to a strongly disordered state in which the correlation function turns negative for large distances. This latter state usually has a slightly lower energy. In certain cases the system again flips back to the "normal" state. In Figures (7) and (8) we

show plots of $G(x)$ versus x in the two different states for $\beta/N \approx 0.5$ for $N=24$ and $N=36$. Figures (9) and (10) show the histories of the internal energy indicating the times at which the flips occurred. As we go further into the weak coupling region this strange behaviour disappears, and the correlation function has a normal behaviour albeit with a larger correlation length. We have checked this by performing runs with as many as 48,000 sweeps in very weak coupling.

We emphasize that the non-analyticity discussed above is not very apparent in the behaviour of the internal energy; in fact, one would very likely miss it completely unless one monitors the correlation function. Neither is it a finite-size effect : the region of non-analyticity is the same for $N=12, 24$ and 36 , and disappears completely in weak coupling. As yet we do not have any explanation of this rather strange phenomenon.

One of our original motivations behind this investigation was to check asymptotic freedom for the model and extract values of the mass gap. The correlation function does show some exponential fall-off; however, in the weak coupling region the correlation length was too large to allow for a sensible discussion of scaling. Probably a better idea of the continuum physics may be obtained by using an improved action.

After this work was completed we received a preprint by Aneva et.al.[9] in which it has been shown that the symmetry

in eqn.(5) above may be used to argue that the extra source terms (14) vanish for all couplings.

ACKNOWLEDGEMENTS

This work was initiated at the University of Chicago. The authors thank Steve Shenker and Dan Friedan for helpful conversations. J.B.K. thanks the Research Board of the University of Illinois for large blocks of background computing time on the research CYBER-175. S.R.D. thanks the Enrico Fermi Institute and the Computer Department of Fermilab for use of their VAX computers. S.R.D would also like to thank the Aspen Center for Physics where part of this work was done. The research of J.B.K. was partially supported by the NSF under Grant No. NSF-PHY82-09148. The research of S.R.D. was partially supported by NSF-Contract No. PHY-83-02112.

REFERENCES

1. T.Eguchi and H.Kawai, Phys.Rev.Lett.48 (1982) 1063.
2. G.Bhanot,U.Heller and H.Neuberger, Phys.Lett. 113B (1982) 47. ;G.Parisi, Phys.Lett.112B (1982) 228.; S.R.Das and S.Wadia, Phys. Lett. 117B (1982) 228.; D.Gross and Y.Kitazawa, Nucl.Phys. B206 (1982) 440.; A.A.Migdal, Phys.Lett.116B (1982) 425.
3. A.Gonzales-Arroyo and M.Okawa, Phys.Rev D27 (1983) 2397. ;T.Eguchi and H.Nakayama, Tokyo University Preprint (November,1982).
4. A.A.Migdal, Zh.Eksp.Teor.Fiz.69 (1975) 810. (Sov.Phys.JETP 42(1975)413).
5. J.Kogut,M.Snow and M.Stone, Phys.Rev.Lett. 47 (1982) 1767,;Nucl.Phys. B200[FS4] (1982) 211.
6. H.Neuberger, Phys.Rev.Lett. 48 (1982) 621.
7. F.Green, Phys.Lett.124B (1983) 501.
8. S.R.Das, (to be published)
9. B.Aneva,Y.Brihaye and P.Rossi, CERN Preprint (September 1983)

FIGURE CAPTIONS

- Fig. 1: Internal energies for $N=12$. Typical errors are 0.01
- Fig. 2: Internal energies for $N=24$. Typical errors are 0.02. The crosses represent energy averages in the "abnormal" state.
- Fig. 3: History of internal energy at very weak coupling. Points are block averages over every 500 sweeps.
- Fig. 4: Histories of internal energy for hot and cold starts in the cross-over region for $N=36, \beta/N=0.20$. Points are block averages over every 50 sweeps.
- Fig. 5: Histories of internal energy for hot and cold starts in the cross-over region for $N=36, \beta/N=0.3$ points are block averages over every 100 sweeps.
- Fig. 6: Typical plots of correlation functions for various beta except in the region of non-analyticity. Typical error bars are shown.
- Fig. 7: Correlation functions for the two states in the region of non-analyticity.
- Fig. 8: Correlation functions for the two states in the region of non-analyticity for $N=36, \beta/N=0.52$.
- Fig. 9: History of internal energy for $N=24, \beta/N=0.5$. Points are block averages over every 500 sweeps. Typical errors are 0.02.

Fig. 10: History of internal energy for $N=36, \beta/N=0.52$. Points are block averages over every 500 sweeps. Typical errors are 0.02.

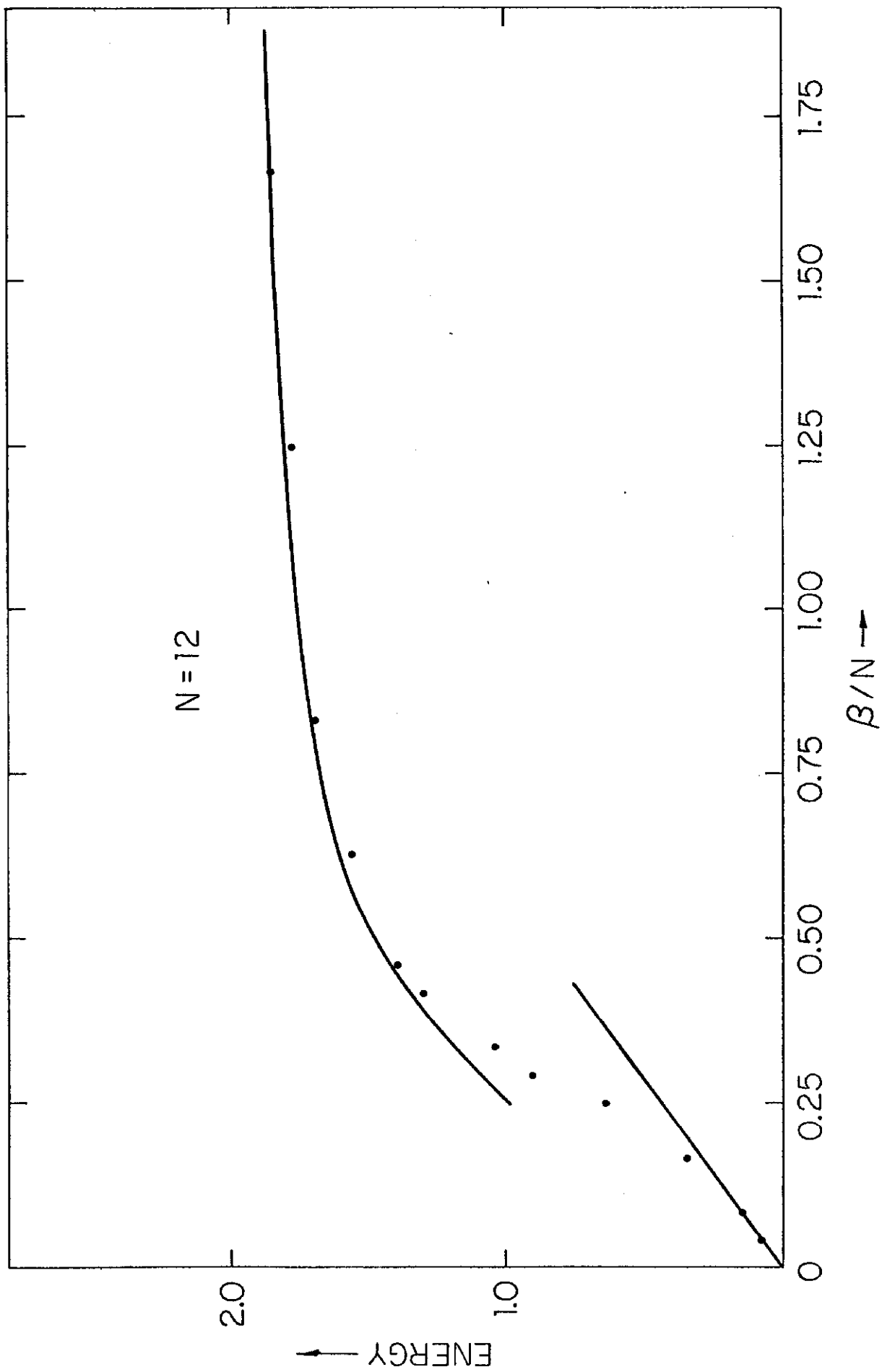


Fig. 1.

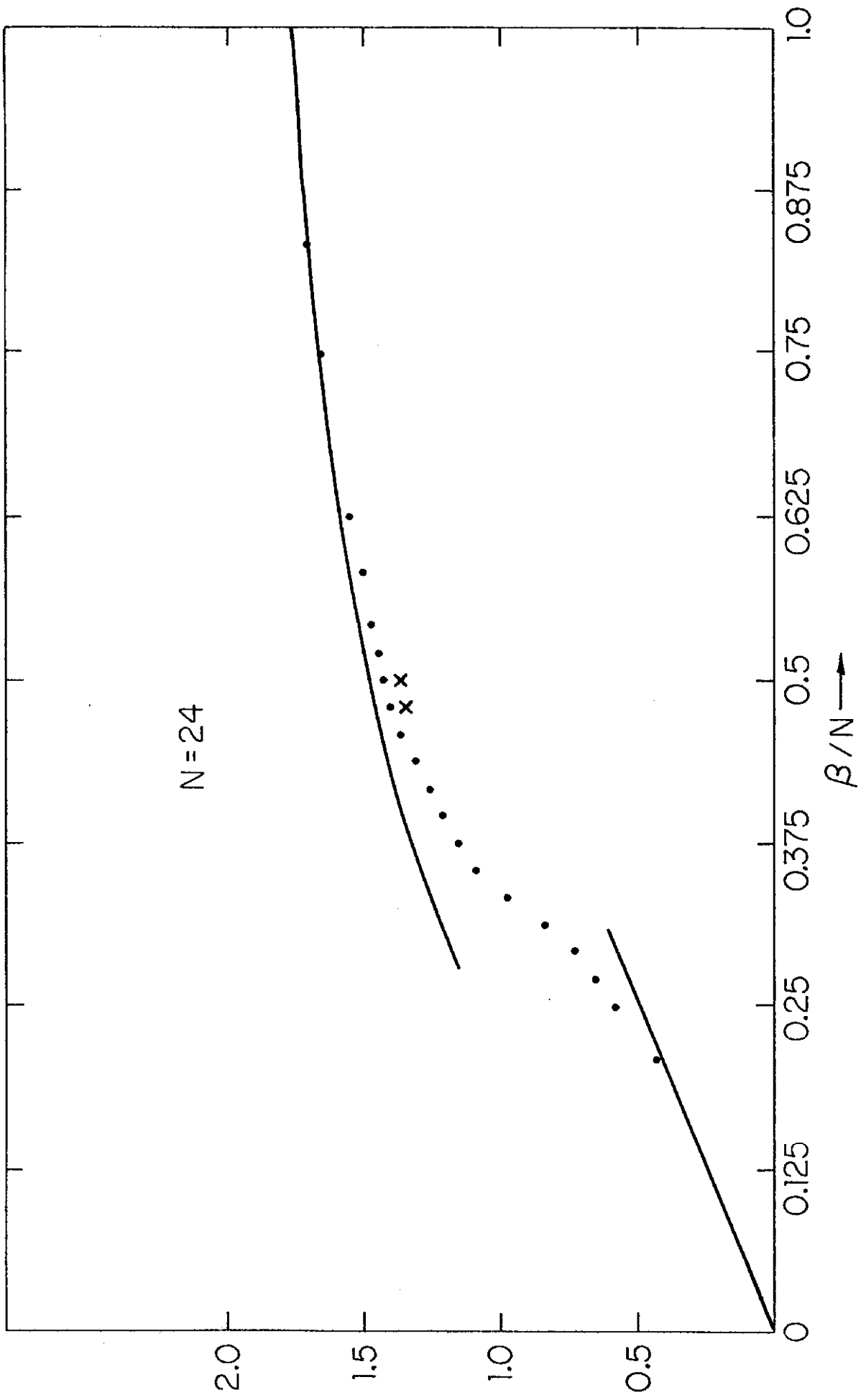


Fig. 2.

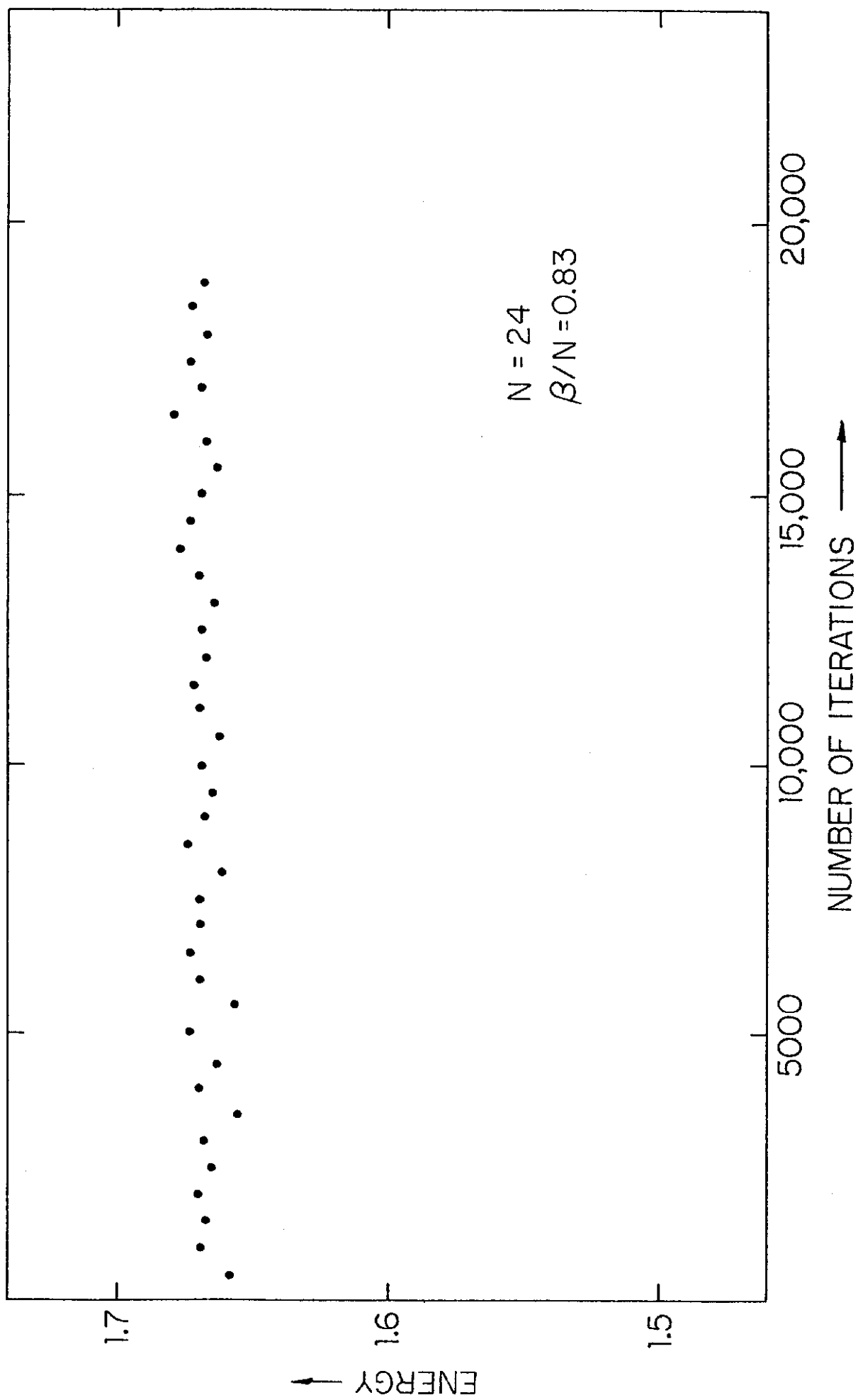


Fig. 3.

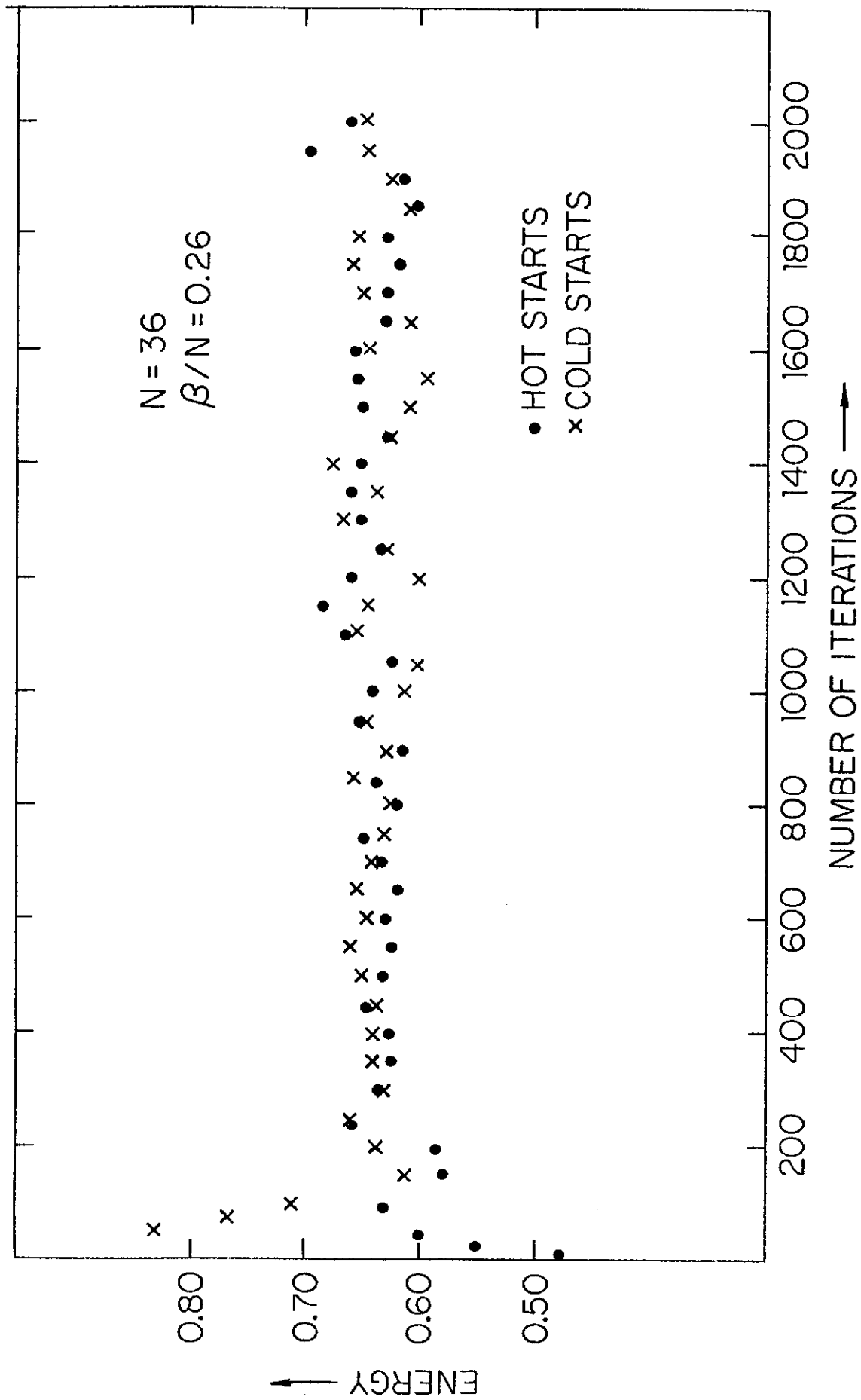


Fig.4.

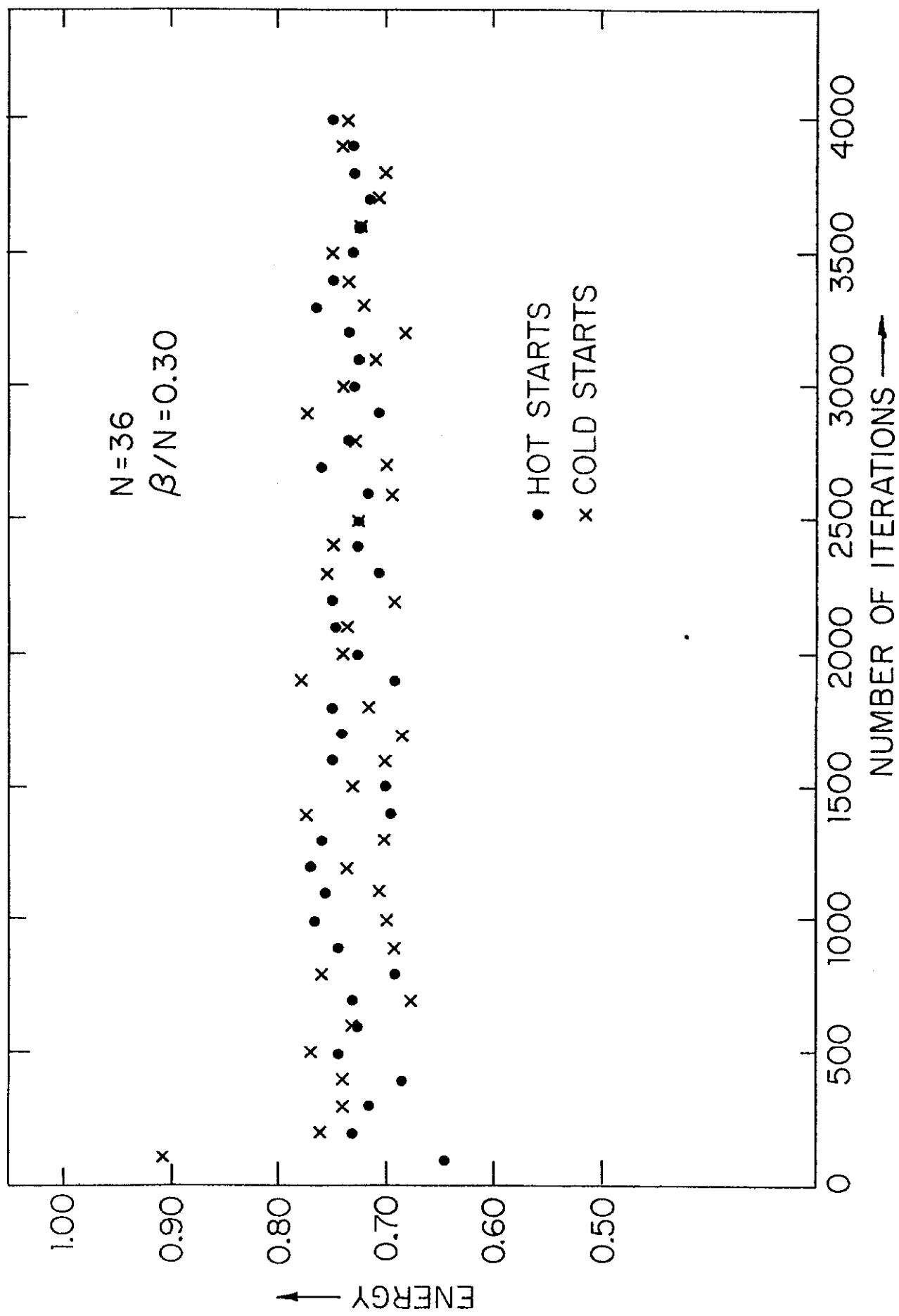


Fig. 5.

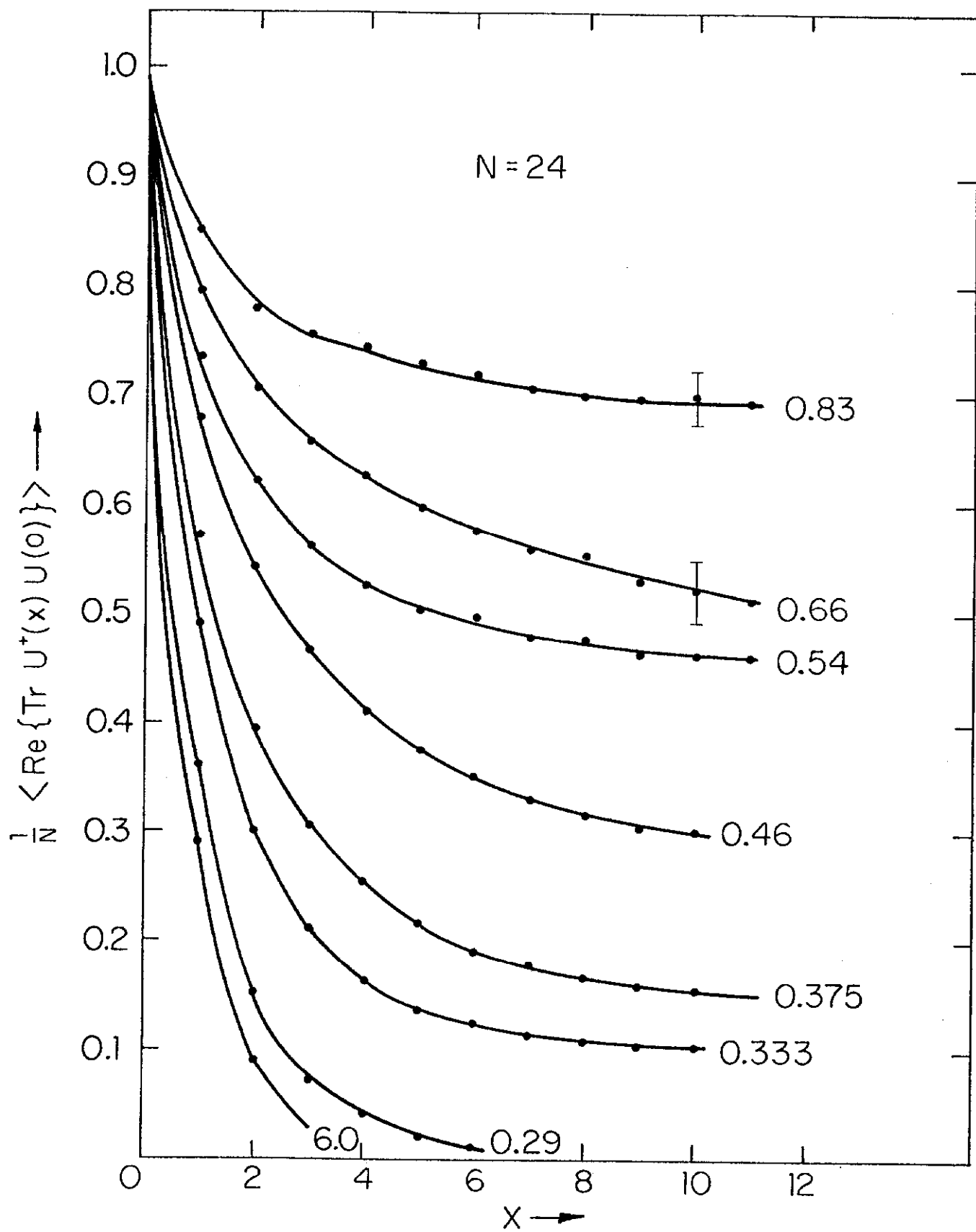


Fig.6.

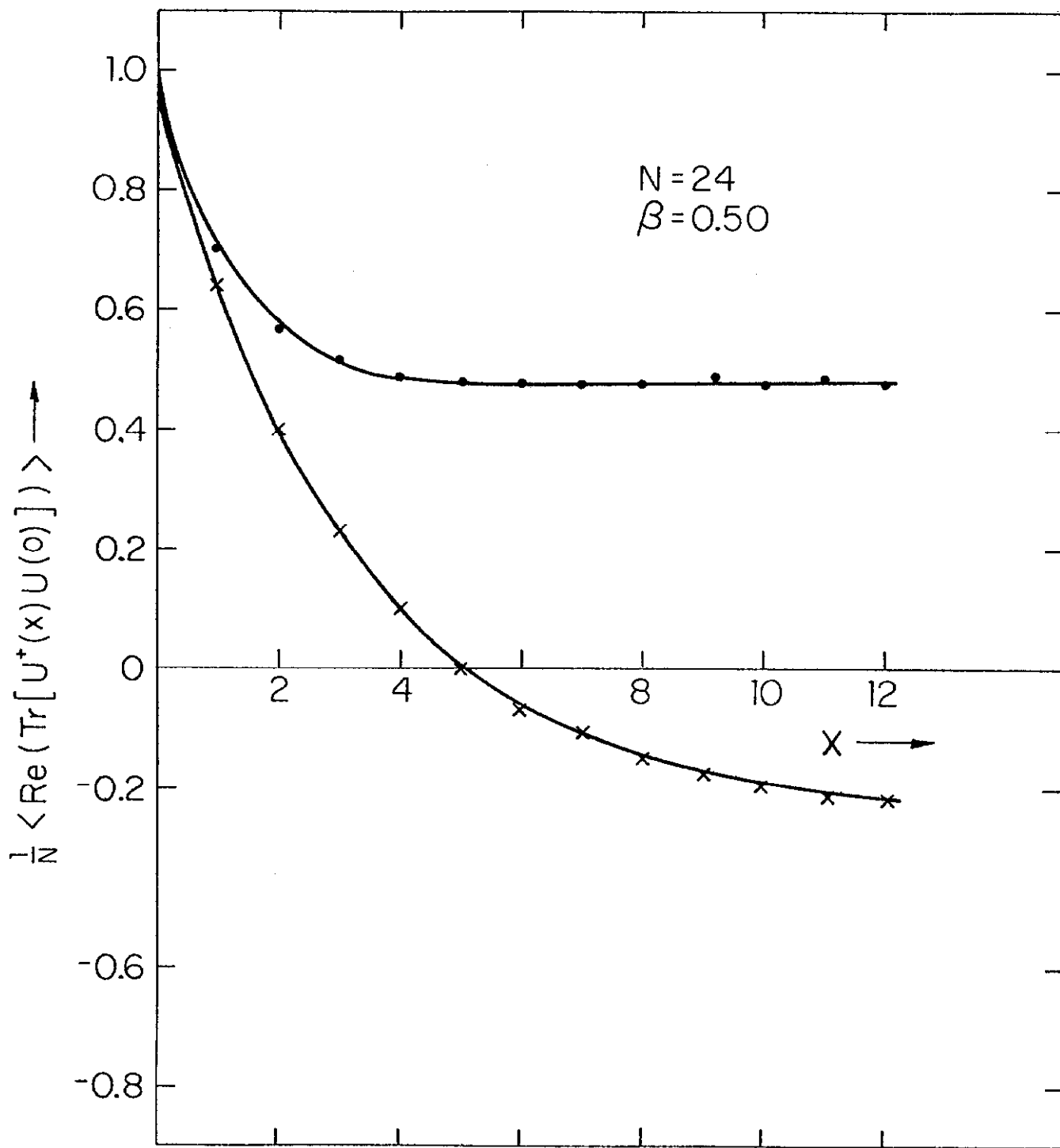


Fig.7.

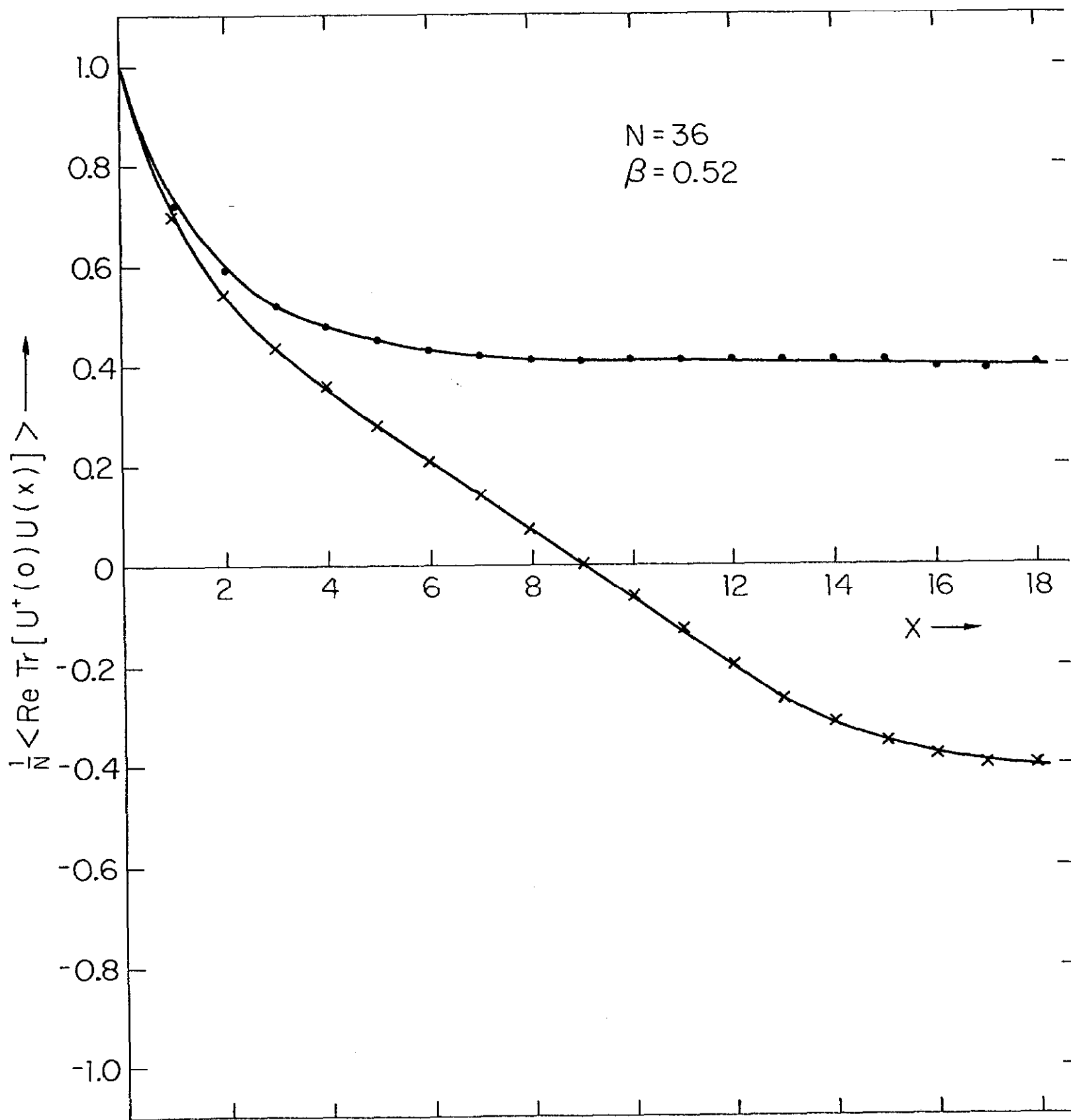


Fig. 8.

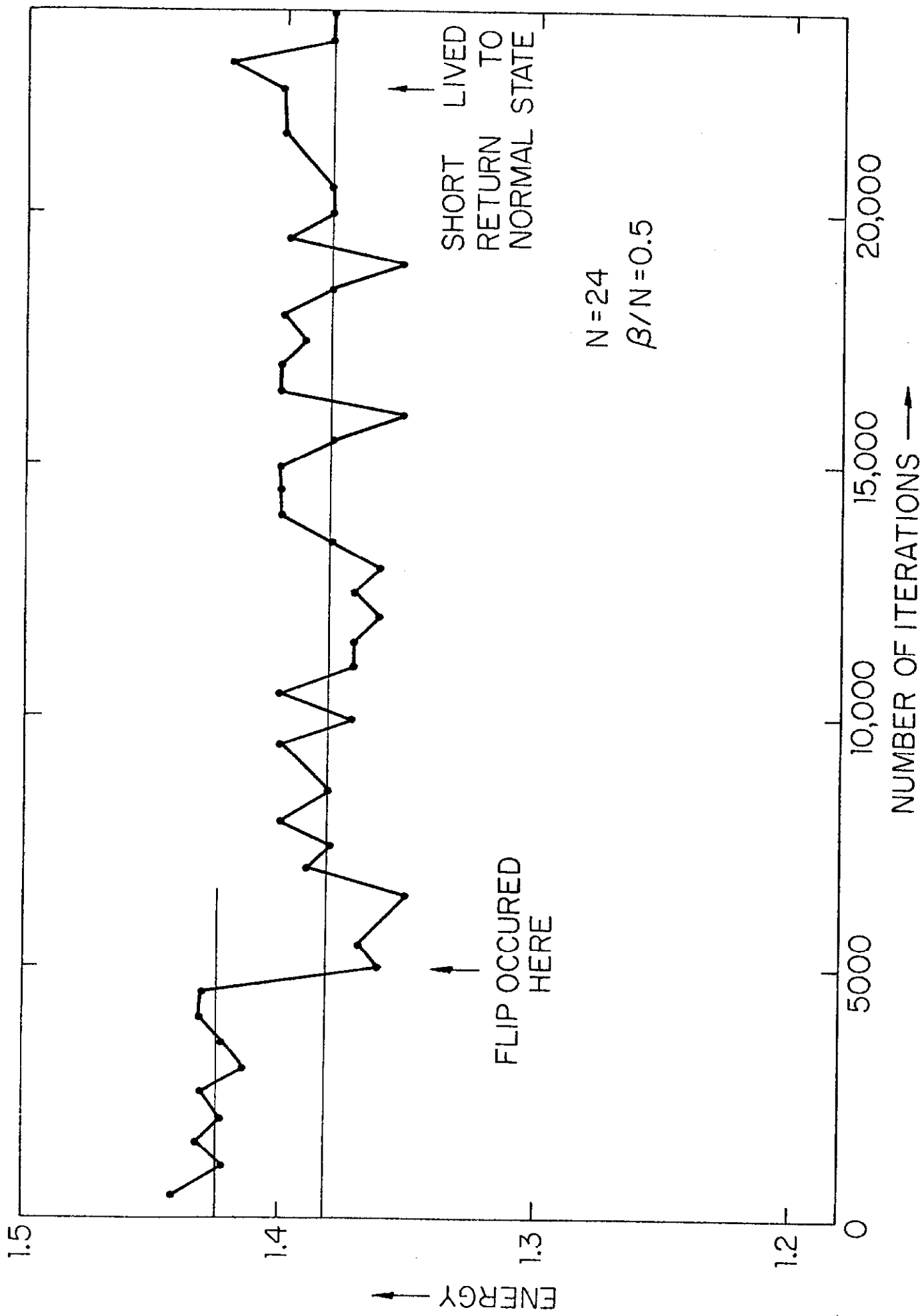


Fig.9.

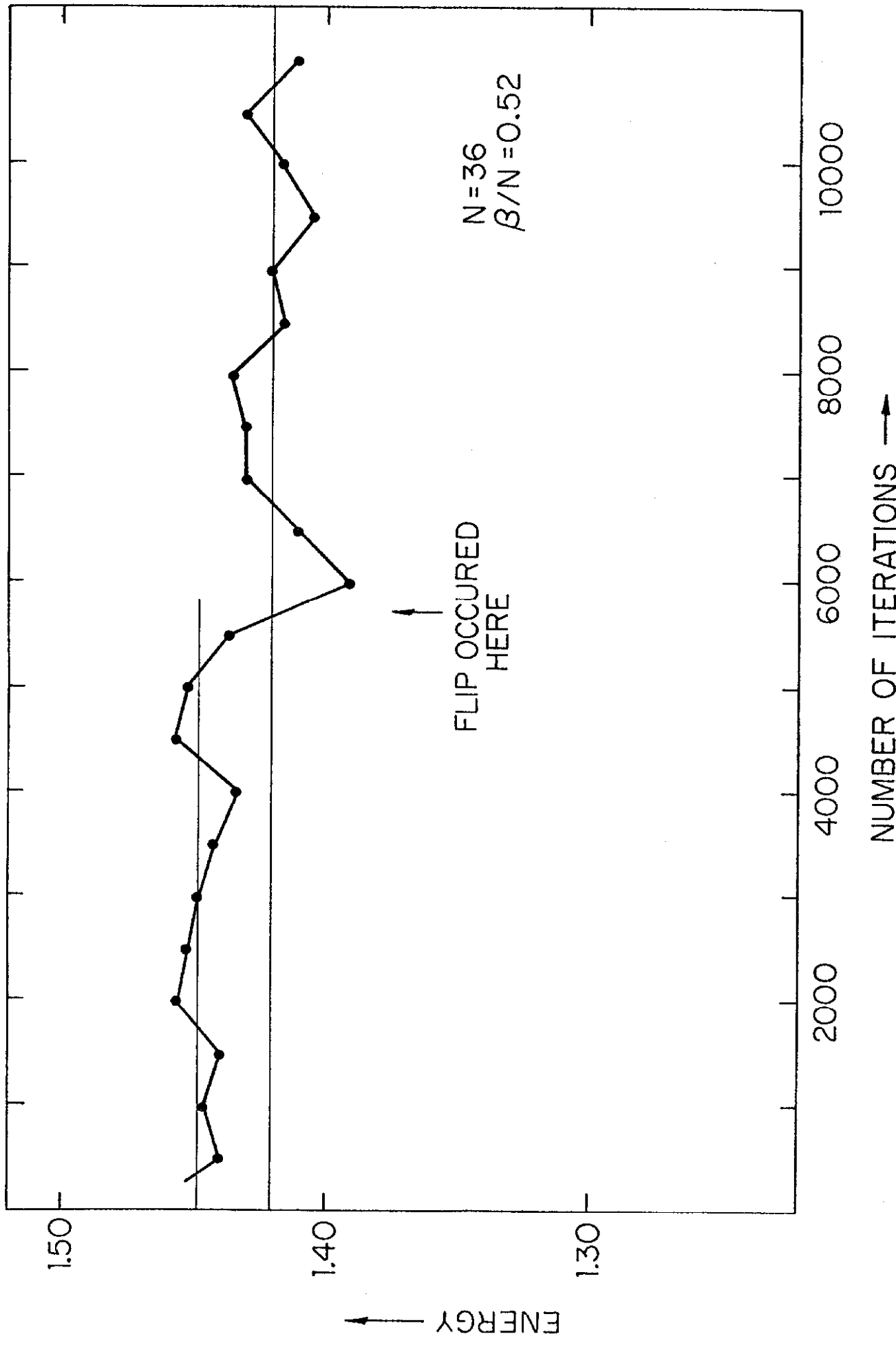


Fig.10.